J Therm Anal Calorim (2015) 121:1049–1057
DOI 10.1007/s10973-015-4520-5

Kinetic of solid-state degradation of transitional coordinative compounds containing functionalized 1,2,4-triazolic ligand

Ionuţ Ledeţi · Gabriela Vlase · Titus Vlase · Vasile Bercean · Adriana Fuliaş

Received: 20 November 2014 / Accepted: 31 January 2015 / Published online: 3 March 2015

Abstract Three coordinative compounds containing Ni(II), Cd(II) and Zn(II) and functionalized 1,2,4-triazolic ligand were prepared and characterized by both thermal and non-thermal methods. The applied instrumental techniques consisted in TG/DTG/HF analysis, FTIR spectroscopy, elemental analysis and complexometric titration, while the decomposition mechanism was evaluated by evolved gas analysis. The kinetic analysis of the thermolysis of the metal complexes was achieved using the thermogravimetric data in air for the main step of decomposition under thermal treatment in non-isothermal conditions. The kinetic parameters were estimated by using three isoconversional methods (Kissinger–Akahira–Sunose, Flynn–Wall–Ozawa and Friedman) and data collected at five different heating rates, $\beta = 5, 7, 10, 12$ and 15 °C min^{-1}. The obtained results were corroborated with the ones obtained by using a different approach of kinetic study, namely the nonparametric kinetics method, which allows a separation of the temperature, respective conversion dependence of the reaction rate. The obtained values for the kinetic parameters are in a good agreement for all the applied protocols.

I. Ledeţi · A. Fuliaş
Faculty of Pharmacy, University of Medicine and Pharmacy "Victor Babeş", Eftimie Murgu Square 2, 300041 Timişoara, Romania

G. Vlase (✉) · T. Vlase
Research Centre for Thermal Analysis in Environmental Problems, West University of Timisoara, Pestalozzi Street 16, 300115 Timişoara, Romania
e-mail: gabriela.vlase@cbg.uvt.ro

V. Bercean
Faculty of Industrial Chemistry and Environmental Engineering, Politehnica University Timişoara, 6 Carol Telbisz, 300001 Timişoara, Romania

Keywords Metal complexes · Functionalized 1,2,4-triazole · Kinetic · NPK method · EGA study

Introduction

Metal complexes gained much attention in various scientific researches, due to their numerous biomedical, technical and agrochemical appliances [1, 2]. The importance of heterocyclic derivatives as pharmacophores, as well as bioactive compounds, is nowadays well known and intensely investigated [3–6]. Among nitrogen-containing heterocycles, 1,2,4-triazoles are studied as pharmacophores in numerous functionalized organic compounds for several well-known biological activities [7–11]. Recent studies indicate that triazoles can be associated with anti-trypanosomal activity [12], nucleotide inhibitors [13] and COX-2 inhibitors [14]. Numerous scientific papers are also reported in the field of metal complexes containing functionalized triazoles as ligands, with and/or without describing their biological activities [15–19]. Supramolecular chemistry of coordinative compounds is a rapidly developing domain in the field of complex combinations aiming towards the design of bioactive and diagnostic agents. Biological activities of coordination compounds created a new class of chemotherapeutic agents for aiming specific physiological and/or pathological targets [20].

The formation of coordinative entities containing as ligand the 1,2,4-triazolic nucleus is in agreement with the structure, existing different binding modes. It is well known that the presence of three endocyclic nitrogens and the possibility of tautomerism [21] may lead to different supramolecular structures. By functionalization of the nucleus by linking to its functional groups that possess complexing capacities, new ligands are obtained. In previous studies

[9–11], we described the functionalization of 1,2,4-triazolic nucleus as well the synthesis of heterocyclic derivatives with potential anti-inflammatory activities as well with a modified complexing capacity. The importance of thermal analysis and its applicability in studying stability of compounds with different structures and roles, along with other instrumental techniques, as well coupled with kinetic studies, was also reported by our research group [22–26].

According to these observations, we set our goal in the synthesis and solid-state characterization of three metal complexes containing a polyfunctionalized S-alkylated triazolic ligand, namely the sodium salt of 4*H*-4-amino-5-carboxymethylsulfanyl-3-phenyl-1,2,4-triazole. Metal complexes were investigated as stoichiometric composition by means of elemental analysis, thermal behaviour, FTIR spectroscopy, complexometric titration and evolved gas analysis.

The kinetic analysis of the degradative process of these metal complexes was investigated using the thermogravimetric data in dynamic air atmosphere for the complex decomposition in non-isothermal conditions (Fig. 1). The non-isothermal experiments were performed at different heating rates, while the data were processed according to an appropriate strategy to the following kinetic methods: Kissinger–Akahira–Sunose, Flynn–Wall–Ozawa, Friedman and NPK, in order to determine realistic kinetic parameters, even if the thermolytic process is a complex one.

Materials and methods

Starting reagents were commercial products (CdI_2, $NiCl_2{\cdot}6H_2O$ and $ZnCl_2$) and used without purification. Synthesis and complete characterization of acid form of the ligand were elsewhere reported [9].

Thin-layer chromatography was carried out on silica gel-coated plates $60F_{254}$ Merck using as eluants three mixtures of solvents, with different polarities, namely benzene/ethyl acetate 1:1 (v/v), benzene/methanol 7:3 or benzene/methanol 3:7.

The composition of the metal complex (C, H and N) was obtained by means of elemental analysis using a VarioEL, Elementar Analysensysteme GmbH. The metal content from metal complexes was determined after desegregation of complexes by complexometric titration, by standard analytical procedures.

Thermoanalytical data TG/DTG/HF were recorded for all samples of masses in the range of 3–7 mg in open aluminium crucibles. Data were drawn up in dynamic air atmosphere (100 mL min^{-1}) at different heating rates $\beta = 5, 7, 10, 12$ and 15 °C min^{-1}, by heating from ambient up to 550 °C, using PerkinElmer DIAMOND equipment.

The evolved gas analysis (EGA) was carried out by a hyphenated TG/FTIR technique, using a PerkinElmer SPECTRUM 100 device with an IR gas chamber connected by a transfer line to the exit of the DIAMOND furnace. The air flow of 100 mL min^{-1} and a heating rate of 20 °C min^{-1} were used. The FTIR spectra were processed by the Sadtler Gas Vapor Library.

The FTIR spectra of different solid samples were obtained on the same spectrometer using the UATR technique.

Results and discussion

The preparation of sodium salt of 4*H*-4-amino-5-carboxymethylsulfanyl-3-phenyl-1,2,4-triazole (1) was realized in aqueous medium by a previously reported procedure followed for the synthesis of Cu(II) [27] and Co(II) complexes [28].

Bivalent metal complexes were prepared by dripping, under intense stirring, an aqueous solution of the ligand to an aqueous solution of metal salt in molar ratio 2:1. After 3 h of continuous stirring, TLC was carried out for the reaction mixture, in order to determine the presence of

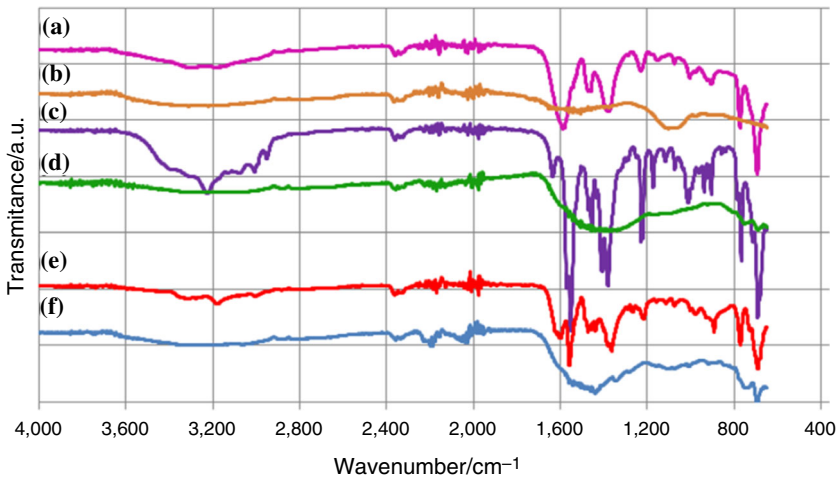

Fig. 1 UATR–FTIR spectra on 4,000–600 cm^{-1} spectral range before thermolysis, for the metal complexes: *a* Ni(II), *c* Cd(II) and *e* Zn(II) and after *c* thermal treatment at 550 °C: *b* Ni(II), *d* Cd(II) and *f* Zn(II), corresponding to metallic oxides

unreacted ligand. In all cases, independently of polarity of eluting solvent, the characteristic spot of ligand was not observed, confirming that a coordinative compound of metal/ligand ratio 1:2 was obtained.

Solid metal complexes were filtered under reduced pressure, washed with distilled water, and dried for 48 h at 30 °C, according to the Scheme 1.

Metal complexes were obtained from the sodium salt of 4*H*-4-amino-5-carboxy-methylsulfanyl-3-phenyl-1,2,4-triazole (L^-Na^+) by the interaction in aqueous medium of the ligand with the solution containing the divalent cation, according to Scheme 1. Metal complexes precipitated instantly after completing the dripping of the ligand. The composition of the metal complex was evaluated by both thermal analysis and elemental analysis, which consisted in both complexometric titrations for determining the metal content, as well the C, H and N by instrumental means. The obtained results are presented in Table 1.

FTIR spectroscopy

The drawing up of the UATR–FTIR spectra for the metal complexes reveals that the formation of coordinative compounds for all three analysed metals occurs by the participation of the ligand in the deprotonated form, through carboxylate moiety. We previously reported the FTIR spectra of the free ligand in both acid form and two metal complexes [27, 28]. The analysis of the spectral range 4,000–2,000 cm^{-1} reveals information about the content of water in the structure of metal complexes, broad bands being observed in all three cases of analysed samples, as follows: for Ni(II) complex, between 3,620 and 2,800 cm^{-1}, with a maximum at 3,334 cm^{-1}; for Cd(II) complex, between 3,600 and 2,800 cm^{-1}, with a maximum at 3,235 cm^{-1}; and for Zn(II) complex, between 3,600 and 2,750 cm^{-1}, with a maximum at 3,318 cm^{-1}. These results are also in good agreement with the ones obtained by EGA study and elemental analysis. The above-mentioned spectral region reveals information about the presence of CH_2 moieties in the structure, as C–H stretches between 2,953 and 2,870 cm^{-1}, for all complexes (Fig. 1).

According to references from already published data [29–32], –COOH group is characterized by two major ways of vibrations: ν(C = O) and ν(C–OH), the last one being represented by two distinctive bands. With the loss of the proton from –COOH moiety, the carboxylate group $-COO^-$ adopts a C_{2v} symmetry, so two distinctive vibrations ν^{as}(COO) and ν^{s}(COO) are expected to be noticed. UATR–FTIR analysis reveals the shifting of ν(C = O) from 1,714 cm^{-1} in the case of free ligand [28] to lower frequencies for all analysed complexes, as follows: 1,555 cm^{-1} for Cd(II), 1,591 cm^{-1} for Ni(II) and 1,625 cm^{-1} for Ni(II) coordination compounds. The formation of the metal complex is sustained by the appearance of new bands in the 600–450 cm^{-1} spectral region, comparative to free ligand bands which can be assigned to ν(Metal → O) and ν(Metal → N), respectively (Fig. 2) [27, 28].

Thermal analysis

The thermoanalytical curves TG/DTG/HF for the three new metal complexes with Cd(II), Ni(II) and Zn(II) are presented in Fig. 3a, b, c. These curves obtained in

Scheme 1 Synthesis of coordinative compounds and structure of ligand

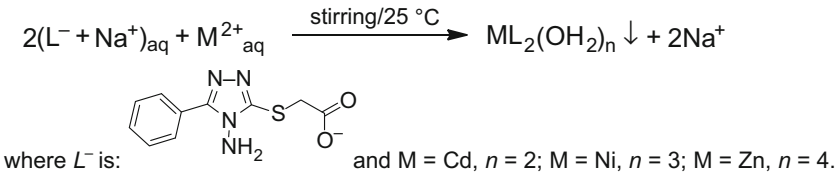

Table 1 Results obtained for the investigation of metal complexes

Results found/calculated	Metal complex		
	$CdL_2(OH_2)_2$	$NiL_2(OH_2)_3$	$ZnL_2(OH_2)_4$
Aspect	White powder	Pale blue powder	Grey powder
Elemental analysis	C: 36.98/37.13	C: 38.96/39.30	C: 37.14/37.77
	H: 3.29/3.43	H: 4.01/3.96	H: 4.31/4.12
	N: 17.11/17.32	N: 18.42/18.33	N: 17.56/17.62
Metal content	16.98/17.37	9.12/9.60	9.96/10.28
Molar mass	643.7/646.98	607.2/611.28	631.1/635.98
Composition formula	$C_{20}H_{22}CdN_8O_6S_2$	$C_{20}H_{24}N_8NiO_7S_2$	$C_{20}H_{26}N_8O_8S_2Zn$

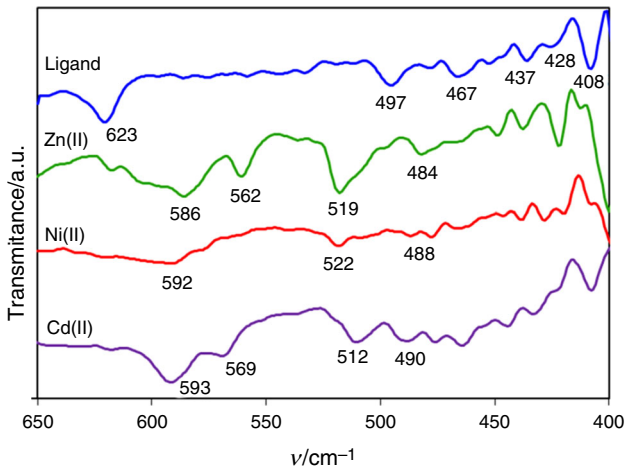

Fig. 2 UATR–FTIR spectra on 650–400 cm^{-1} spectral range for ligand and metal complexes

dynamic air atmosphere showed that these compounds decompose during several processes which have a different nature (endo- and exothermic steps).

The simultaneous curves TG/DTG/HF for the Cd(II) complex are shown in Fig. 3a. In accordance with HF curve, a sharp endothermic peak is observed at 103.5 °C with a change of the sample mass of $\Delta m = 5.4$ %, corresponding to the dehydration step of hydrated complex. Up to the end of water loss process, the Cd(II) complex is thermally stable up to 187 °C. At higher temperature, this complex presents two main steps with a significant mass loss between 190–380 °C ($\Delta m = 36.8$ %) and 380–550 °C ($\Delta m = 37.8$ %). The DTG curve presents a broad peak in the first temperature range which is accompanied by two peaks on the HF curve with an exothermal nature and maximum at 288 and 330 °C, respectively. The last step has a sharp and important exothermic behaviour ($HF_{max} = 487$ °C) due to the complete thermodegradation of all organic moieties from complex. The final mass obtained during heating is in good agreement with the one expected for the formation of the divalent metallic oxide, CdO (Fig. 1d).

The thermal decomposition of Ni(II) complex exhibited three mass loss steps (Fig. 3b) attributed to a total degradation of the ligand, with a complete mass loss until a constant mass representing NiO as final product (Fig. 1b). The thermogravimetric curve reveals a water loss process beginning from 40 up to 120 °C, when a thermal stability range appears up to 215 °C which is the decomposition onset temperature of the Ni(II) complex. The mass loss found in the dehydration temperature range is practically equal with the calculated water content.

In the case of Zn(II) complex (Fig. 3c), the first thermal event was observed starting at ≈45 °C, with two maxima on HF curve, at 98 and 178 °C, respectively. These steps

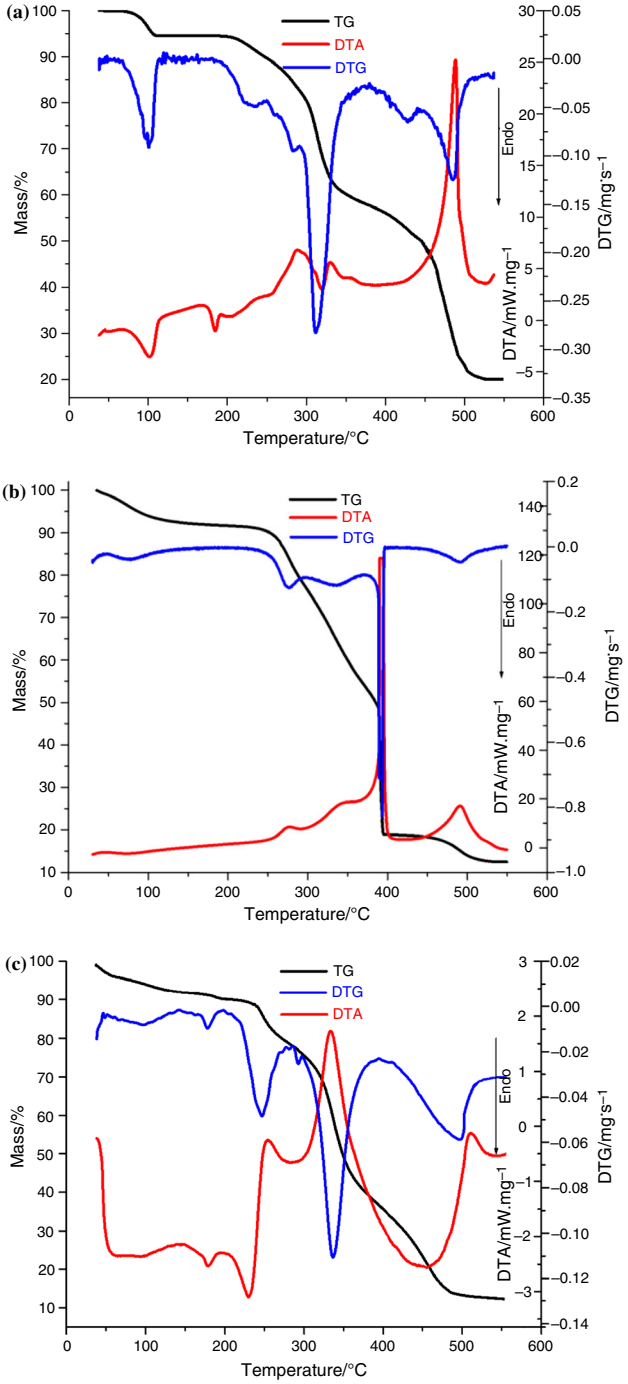

Fig. 3 Thermoanalytical curves for samples of complexes with **a** Cd(II), **b** Ni(II) and **c** Zn(II) recorded in air atmosphere with a heating rate $\beta = 7$ °C min^{-1}

are accompanied by a total mass loss $\Delta m = 11.0$ %. According to the HF curve, the first process is a two-step dehydration, indicating the loss of 4 mol of water per mol of complex. By the analysis of temperature range corresponding to water loss, 2 mol correspond to lattice water and 2 mol to coordination water. The dehydration process is followed by a continuos degradation, revealed by three

Table 2 Thermoanalytical data of the analysed complexes

Complex	Process	T_i/°C	T_f/°C	$T_{max\ DTG}$/°C	$T_{max\ HF}$/°C	Δm/%
$ZnL_2(OH_2)_4$	I	45	200	95; 177	98; 178	11.0
	II	200	280	247; 336	229; 252; 332	12.1
	III	280	400	336	334	41.7
	IV	400	550	502	510	22.2
$NiL_2(OH_2)_3$	I	40	120	101	102	9.0
	II	215	300	275	278	15.1
	III	300	370	330	345	22.2
	IV	370	400	395	397	34.7
	V	445	550	490	488	7.0
$CdL_2(OH_2)_2$	I	68	114	102.8	103.5	5.4
	II	187	380	312	184; 288; 330	36.8
	III	380	550	486	487	37.8

consecutive peaks (one endothermic and two exothermic) with maximums at HF_{max}= 229; 252 and 332 °C, respectively. The final mass obtained is identified as ZnO (Fig. 1f). During these three steps, a continuous mass loss was observed on TG curve, the kinetic analysis being performed on the first degradation step between 200 and 286 °C, respectively, with DTG_{max} = 245 °C.

The last process is attributed to the advanced oxidation of the fragments from ligand, followed by a complete destruction of organic skeletons, and following this, an intense exothermic event on the HF curve is observed. The distinction between the three thermal degradations is that the Ni(II) complex shows a very strong exothermic effect for the last process on HF curve.

Table 2 presents the summarized data of all thermal events (temperature ranges, peak temperatures and mass losses), as revealed by the thermoanalytical curves.

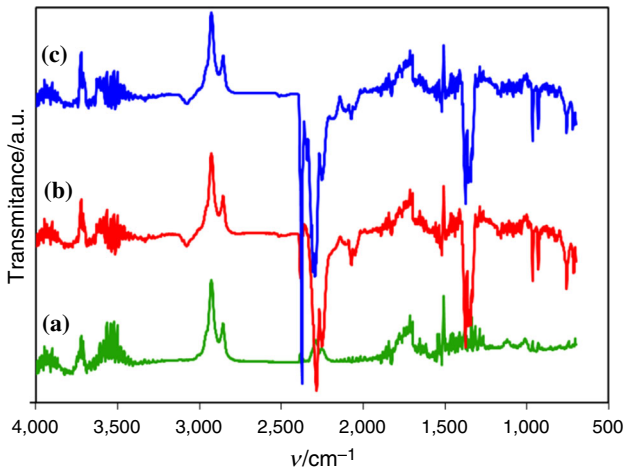

Fig. 4 FTIR profile for mixture from EGA: Ni(II) complex at: *a* 11.7 min, *b* 13.3 min, *c* 13.9 min

EGA study

The thermal degradation of the metal complexes in oxidative atmosphere was monitored by the analysis of evolved gases using a coupled FTIR spectrometric gas cell as a detector, directly connected to the furnace of thermal balance (Figs. 4, 5, 6). The components of released gaseous mixtures have been monitored and identified on the basis of their FTIR spectra, from Gram–Schmidt profile and thermogravimetric curves recorded at a heating rate $\beta = 20$ °C min^{-1}. The main gaseous species that can be identified from the FTIR-EG spectra are water vapours (ν = 3,750–3,500 and 1,900–1,300 cm^{-1}) in all cases and at decreased times and temperatures, confirming that the water loss occurs in first decomposition stages. The results obtained from the EGA study are in good agreement with the ones suggested by the thermoanalytical curves, regarding both dehydration step and the final residue (Table 3).

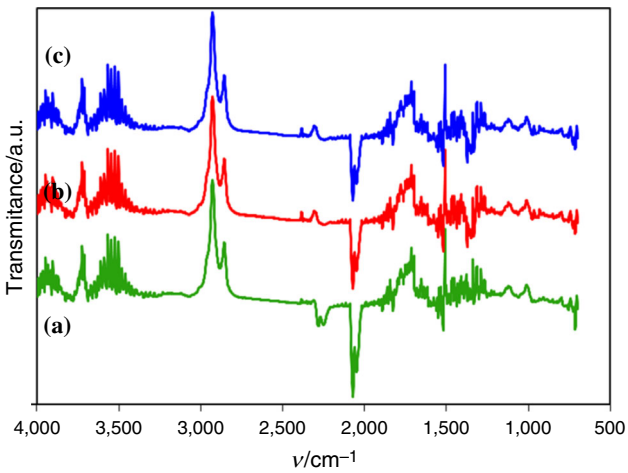

Fig. 5 FTIR profile for mixture from EGA: Cd(II) complex at *a* 13.7 min, *b* 15.2 min, *c* 15.7 min

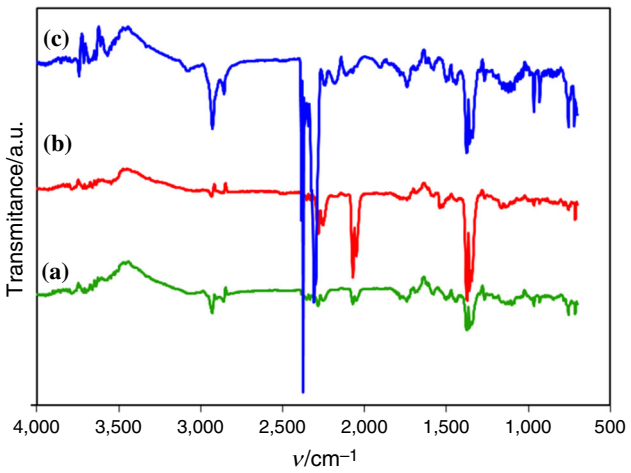

Fig. 6 FTIR profile for mixture from EGA: Zn(II) complex at *a* 11.2 min; *b* 12.0 min; *c* 12.6 min

Table 3 Correlation between experimental and calculated data for dehydration step and final residue

	Δm dehydration/%		Δm final residue/%	
	Experim.	Calc.	Experim.	Calc.
$ZnL_2(OH_2)_4$	11.0	11.32	13.0	12.80
$CdL_2(OH_2)_2$	5.4	5.56	20.0	19.84
$NiL_2(OH_2)_3$	9.0	8.83	12.0	12.22

Because the EGA was carried out on a temperature higher than that of one of the study processes, in the IR spectra other bands were observed, as expected. This is another confirmation that the degradative process is continuous with the increase in the temperature. A similar EGA profile was observed for the decomposition products on temperatures below 400 °C. With the increase in the temperature up to 490 °C, in the IR spectrum new bands appeared. The main compound that can be identified from the EGA spectrum is carbon dioxide ($\nu = 2{,}372$ cm^{-1}). The fact that the decarboxylation occurs at such a high temperature can be explained by the fact that the carboxyl group is involved in the coordinating bond and that the lateral heterocyclic moiety is more susceptible to degradation, just like in the case of other metal complexes [27]. The intense bands around 3,000 cm^{-1} are associated with aromatic C–H from benzene, which is released after destruction of lateral moieties from ligand. The bands around 1,950–1,800 cm^{-1}, as well the ones around 1,650–1,550 cm^{-1} with hyperfine structure, are associated with the absorbance of nitrous oxide, which is an oxidation product of nitrogen from endocyclic triazole and/or amino group. Other bands, associated with the presence of dimethyl sulphide, appear around 1,437, 1,408, 1,310, 1,057 and 955 cm^{-1} at high temperatures and suggest the breakdown of the triazolic nucleus in the nearby of the S-moiety.

Kinetic study

The thermal degradation of the anhydrous complexes containing the same triazolic ligand and different metal cation suggests a stability order of Cd(II) < Zn(II) < Ni(II) ($T_{\text{onset}} = 187 < 200 < 215$ °C). In order to confirm this order of stability, a kinetic study was performed for the decomposition processes starting at the above-mentioned temperatures.

The non-isothermal kinetic studies were performed by application of two isoconversional integral methods: Flynn–Wall–Ozawa (FWO) and Kissinger–Akahira–Sunose (KAS), and a differential one, Friedman (FR). For a complete analysis of the kinetic study, a method that does not use any approximation was applied, namely the NPK method. The kinetic analysis was performed on DTG data, in order to determine the characteristic kinetic parameters of the decomposition process, namely activation energy E_a and pre-exponential factor A. Thermoanalytical curves were recorded under heating rates $\beta = 5$, 7, 10, 12 and 15 °C min^{-1} in air atmosphere under dynamic flow, and data were analysed for decomposed fraction α from 0.05 to 0.95 with a step of 0.05.

Isoconversional methods (IM)

IM are based on determining the temperature values for constant degree of conversion (α) while carrying out the

Table 4 Applied isoconversional methods for kinetic analysis

Kinetic method	Equation	Approximation	Graphical representation
Friedman (FR) [33]	$\ln[\beta \cdot (\mathrm{d}\alpha/\mathrm{d}T)]_\alpha = \ln[A \cdot f(\alpha)] - E_a/(RT)$	Differential form	$\ln[\beta \cdot (\mathrm{d}\alpha/\mathrm{d}T)]_\alpha = f(1/T_\alpha)$
Flynn–Wall–Ozawa (FWO) [34, 35]	$(\ln\beta)_\alpha = \ln[A \cdot E_a/R \cdot g(\alpha)] - 5.331 - 1.052 \cdot E_a/(RT)$	Murray and White approximation [36]	$(\ln\beta)_\alpha = f(1/T_\alpha)$
Kissinger–Akahira–Sunose (KAS) [37, 38]	$\ln(\beta/T^2) = \ln[A \cdot E_a/R \cdot g(\alpha)] - E_a/(R \cdot T)$	Doyle approximation [39]	$\ln(\beta/T^2)_\alpha = f(1/T_\alpha)$

analyses at several heating rates β, usually four or five. By using different approximations (Table 1), these methods allow a linear graphical representation of an expression against the reciprocal of the temperature ($1/T$), the last being expressed on Kelvin scale. After linear plotting of data for each method (Table 4), the slopes of the straight lines generate the estimated value of the activation energy, E_a.

The activation energy values were calculated according to the expressions presented in Table 4. The integral isoconversional methods (FWO and KAS) gave similar results with a good confidence revealed by the values of the standard deviation, while the results obtained by applying the Friedman method lead to E_a values being generally higher (in the case of Ni(II) and Cd(II) complexes) than those obtained by integral methods. These differences can be associated with the fact that a different mathematical treatment (a differential one) of the data indicates multistadial process of decomposition.

The values for E_a obtained in non-isothermal conditions for the thermal decomposition of the new metal complexes using decomposed fraction (α) are listed in Table 5.

The nonparametric kinetics method (NPK) initially elaborated by Sempere et al. [40, 41] and modified and developed by Vlase et al. [42, 43] is based on only one assumption that the reaction rate can be written as a product of two independent functions, a function of the degree of conversion [$f(\alpha)$] and a function of temperature [k(T)], according to the equation: $d\alpha/dt = k(T) \cdot f(\alpha)$. Using different values for β, the reaction rates can be expressed as an $n \times m$ matrix which has the rows completed with values obtained at constant conversion degree and whose columns account for the different but constant values of temperature. For the matrix decomposition to obtain two vectors, singular value decomposition (SVD) algorithm [44] was used.

The results of NPK analysis are systematized in Table 6 and were obtained using a kinetic model suggested by Šesták and Berggren [45].

The λ parameter from Table 6 represents explained variance and is defined as the contribution of each step to the whole thermodegradation process, so that $\Sigma \lambda_i = 100$ %.

The results suggested by the obtained values for the activation energies (E_a) for the three analysed complexes are also in good agreement with the ones obtained for the rate constants (k) evaluated by means of NPK method, at the same temperature (250 °C). Also, a reaction rate (r) was evaluated at the same temperature, suggesting the same stability order as the one obtained by the evaluation of E_a and k.

Table 5 Obtained values for activation energies by isoconversional methods for the analysed metal complexes

E_a/kJ mol^{-1}		Conversion degree α																		$\bar{E}_a$/kJ mol^{-1}
		0.05	0.1	0.15	0.2	0.25	0.3	0.35	0.4	0.45	0.5	0.55	0.6	0.65	0.7	0.75	0.8	0.85	0.9	0.95	
Cd(II) cpx	FR	132.5	130.3	133.2	145.5	153.5	150.3	150.1	150.6	151.9	155.8	147.0	144.3	150.9	145.3	139.1	138.9	145.7	139.8	147.2	144.8 ± 1.7
	KAS	127.5	130.0	136.2	136.1	136.3	141.8	139.2	133.4	143.6	141.3	144.0	144.0	153.2	154.0	151.9	150.9	155.1	134.4	120.2	140.7 ± 2.2
	FWO	129.1	131.7	137.9	138.3	138.3	143.7	141.4	136.0	145.7	143.6	146.2	146.3	154.9	155.8	153.9	152.9	157.0	137.4	124.0	142.8 ± 2.2
Zn(II) cpx	FR	114.3	116.9	119.0	121.3	121.9	122.2	124.9	124.7	123.1	124.0	122.6	122.2	122.0	120.9	120.2	119.8	121.0	122.4	119.1	121.2 ± 0.9
	KAS	117.2	117.9	119.0	119.3	119.9	120.9	121.6	121.3	121.9	123.0	123.6	123.9	123.0	122.7	121.3	121.0	119.3	118.9	117.1	120.7 ± 0.5
	FWO	118.3	118.5	119.9	120.1	121.1	121.7	122.9	123.1	123	124.2	124.7	124.6	124.4	124.2	122.9	122.1	120.7	120.1	118.6	121.9 ± 0.6
Ni(II) cpx	FR	85.5	93.1	104.9	108.1	107.4	100.7	107.6	104.8	105.5	103.0	106.9	104.3	106.3	101.7	106.5	106.6	106.8	110.0	120.6	104.8 ± 1.6
	KAS	81.7	87.8	89.6	90.5	91.5	88.6	89.4	91.0	92.9	94.1	98.3	98.5	101.0	101.0	102.8	102.9	103.0	106.3	117.5	96.2 ± 1.9
	FWO	85.9	91.8	93.6	94.5	95.5	92.6	93.6	95.2	97.0	98.2	102.2	102.4	104.8	104.8	100.1	101.8	97.6	99.9	101.8	97.5 ± 1.2

Table 6 Results obtained by the NPK method

	Process	λ/%	E/kJ mol^{-1}	A/min^{-1}	n	m	Šestak–Berggren Eq. $g(\alpha) = (1-\alpha)^n \cdot \alpha^m$	λE/kJ mol^{-1}	k_{250}/min^{-1}	r_{250}/min^{-1}
Cd(II) complex	1	73	160.3 ± 9.1	7.33×10^{11}	1	–	$(1-\alpha)$	156.3 ± 10.4	5.7×10^{-4}	2.9×10^{-4}
	2	27	145.8 ± 6.9	6.65×10^{12}	1	3/2	$(1-\alpha) \cdot \alpha^{3/2}$			
Ni(II) complex	1	87.8	92.8 ± 5.3	3.09×10^{8}	1	–	$(1-\alpha)$	96.7 ± 5.1	7.6×10^{0}	1.2×10^{-1}
	2	12.2	125.0 ± 9.2	2.81×10^{11}	1	2	$(1-\alpha) \cdot \alpha^{2}$			
Zn(II) complex	1	91.6	118.4 ± 10.2	6.13×10^{9}	1	–	$(1-\alpha)$	119.5 ± 7.1	5.9×10^{-2}	5.3×10^{-3}
	2	8.1	136.1 ± 5.1	5.55×10^{11}	–	1	α			

Conclusions

All analysed samples present the first mass loss between 40 and 120 °C [Ni(II) complex] and around 180 °C [Cd(II) and Zn(II) complexes], respectively, due to the dehydration process. The TG curves show that the anhydrous complexes are stable up to a considerable high temperature (approximately 200 °C). After dehydration, the mass loss occurs, in case of all samples, due to the thermal decomposition of the organic ligand in consecutive and overlapped steps which are the same for each metal complex.

The similarity between the infrared spectra in the 2,000–650 cm^{-1} range suggests that in all of the complexes, the ligand is bound in the same mode, and the difference observed in 3,600–2,800 cm^{-1} range is due to the presence of water in different quantity and bounding. Solely in the case of Zn(II) complex, the four water molecules can be tentatively associated with lattice water (two molecules) and with coordination water (two molecules). For Ni(II) and Cd(II) complexes, the overlapping processes of water loss make harder to assume the nature of water molecules.

Using the DTG data at five heating rates, the activation energy associated with the degradation of these structures was evaluated by isoconversional methods, namely Friedman, KAS and FWO, as well by the use of the NPK method. The trend in the variation of activation energies calculated for the thermolysis of triazolic complexes by employing integral methods is in good agreement. The differences obtained by Friedman method resides mainly in the differential processing of the data. Solely the NPK method led to evaluation of the kinetic parameters without a priori approximation. All kinetic methods—both isoconversional and NPK—led to the values of the activation energy which are comparable, confirming the validity of the obtained results.

The main important conclusion of the study resides in the fact that solely thermal analysis as TG/DTG data is not the most valuable tool in analysing the stability of a chemical entity, as long as the results are not correlated with a kinetic study. In our case, TG data suggested that the stability of the complexes decreases in the order Cd(II) < Zn(II) < Ni(II) and that while performing the kinetic analysis, the order is reversed: Cd(II) > Zn(II) > Ni(II). These results were also sustained by the data obtained for rate constants and reaction rates, evaluated at the same temperature for all three metal complexes.

Acknowledgements This work was supported by a Grant from the University of Medicine and Pharmacy "Victor Babeş" Timişoara (Grant II-C2-TC-2014-16498-08 to Ionuţ Ledeţi).

References

1. Lo KK-W, Li SP-Y. Utilization of the photophysical and photochemical properties of phosphorescent transition metal complexes in the development of photofunctional cellular sensors, imaging reagents, and cytotoxic agents. RSC Adv. 2014;4(21):10560–85.
2. Giannousi K, Avramidis I, Dendrinou-Samara C. Synthesis, characterization and evaluation of copper based nanoparticles as agrochemicals against *Phytophthora infestans*. RSC Adv. 2013;3(44):21743–52.
3. Kaushik NK, Kaushik N, Attri P, Kumar N, Kim CH, Verma AK, Choi EH. Biomedical importance of indoles. Molecules. 2013;18(6):6620–62.
4. Harmatova Z, Jona E, Medvecka J, Valigura D, Mojumdar SC. Thermal properties of solid complexes with biologically important heterocyclic ligands. J Therm Anal Calorim. 2014;. doi:10.1007/s10973-014-4114-7.
5. Mojumdar SC, Melnik M, Jona E. Thermal and spectral properties of Mg(II) and Cu(II) complexes with heterocyclic N-donor ligands. J Anal Appl Pyrolysis. 2000;53:149–60.
6. Pajtasova M, Ondrusova D, Jona E, Mojumdar SC, Lalikova S, Bazylakova T, Gregor M. Spectral and thermal characteristics of cooper (II) carboxylates with fatty acid chains and their benzothiazole addicts. J Therm Anal Calorim. 2010;100:769–77.
7. El-Gammal OA, Abu El-Reash G, Ahmed SF. Synthesis, spectral characterization, molecular modeling and in vitro antibacterial activity of complexes designed from O2, NO and NO donor Schiff-base ligand. Spectrochim Acta A. 2015;135:417–27.
8. Ledeti I, Fulias A, Vlase G, Vlase T, Bercean V, Doca N. Thermal behaviour and kinetic study of some triazoles as potential anti-inflammatory agents. J Therm Anal Calorim. 2013;114:1295–305.

9. Ledeti IV, Bercean VN, Badea V, Balan M, Csunderlik C. The Alkylation of 1*H*-5-mercapto-3-phenyl-1,2,4-triazole and 4*H*-4-amino-5-mercapto-3-phenyl-1,2,4-triazole. Rev Chim-Bucharest. 2010;61(9):833–7.
10. Bercean VN, Ledeti IV, Badea V, Balan M, Csunderlik C. New heterocyclic tioether derived from 3-substituted-4*H*-4- amino-5-mercapto-1,2,4-triazoles and succinic acid. Rev Chim-Bucharest. 2010;61(11):1028–30.
11. Ledeti IV, Bercean VN, Tanase IM, Creanga AA, Badea V, Csunderlik C. New azomethine derivatives of 3-substituted-4H-4-amino-5-Ethoxycarbonyl-methylsulfanyl-1,2,4-triazoles as potential anti-inflammatory agents. Rev Chim-Bucharest. 2010; 61(10):935–7.
12. Papadopoulou MV, Bloomer WD, Rosenzweig HS, Wilkinson SR, Kaiser M. Novel nitro(triazole/imidazole)-based heteroarylamides/sulfonamides as potential antitrypanosomal agents. Eur J Med Chem. 2014;87:79–88.
13. Khan KM, Siddiqui S, Saleem M, Taha M, Saad SM, Perveen S, Choudhary MI. Synthesis of triazole Schiff bases: novel inhibitors of nucleotide pyrophosphatase/phosphodiesterase-1. Bioorgan Med Chem. 2014;22:6509–14.
14. Abuo-Rahma GEDAA, Abdel-Aziz M, Farag NA, Kaoud TS. Novel 1-[4-(Aminosulfonyl)phenyl]-1H-1,2,4-triazole derivatives with remarkable selective COX-2 inhibition: design, synthesis, molecular docking, anti-inflammatory and ulcerogenicity studies. Eur J Med Chem. 2014;83:398–408.
15. Gaber M, El-Ghamry H, Atlam F, Fathalla S. Synthesis, spectral and theoretical studies of Ni(II), Pd(II) and Pt(II) complexes of 5-mercapto-1,2,4-triazole-3-imine-2′-hydroxynaphyhaline. Spectrochim Acta A. 2015;137:919–29.
16. Berezovskii GA, Bushuev MB, Pishchur DP, Lavrenova LG. Heat capacity of polynuclear $Fe(HTrz)_3(B_{10}H_{10})$ H_2O and trinuclear $[Fe_3(PrTrz)_6(ReO_4)_4(H_2O)_2](ReO_4)_2$ complexes (HTrz = 1,2,4-triazole, PrTrz = 4-propyl-1,2,4-triazole) manifesting 1A1⇔5T2 spin transition. J Therm Anal Calorim. 2008;93:999–1002.
17. Badea M, Olar R, Marinescu D, Vasile G. Thermal behavior of some new triazole derivative complexes. J Therm Anal Calorim. 2008;92:209–14.
18. Calu L, Badea M, Chifiriuc MC, Bleotu C, David GI, Ioniţă G, Măruţescu L, Lazăr V, Stanică N, Soponaru I, Marinescu D, Olar R. Synthesis, spectral, thermal, magnetic and biological characterization of Co(II), Ni(II), Cu(II) and Zn(II) complexes with a Schiff base bearing a 1,2,4-triazole pharmacophore. J Therm Anal Calorim. 2014;. doi:10.1007/s10973-014-3970-5.
19. Qin J, Lei N, Zhu HL. Synthesis, structural characterization, molecular docking, and urease inhibition studies of dinuclear cobalt(II) complexes derived from 3,5-bis(pyridin-2-yl)-4-amino-1,2,4-triazole. J Coordin Chem. 2014;67:1279–89.
20. Cerchiaro G, Ferreira AMDC. Oxindoles and copper complexes with oxindole-derivatives as potential pharmacological agents. J Braz Chem Soc. 2006;17:1473–85.
21. Yelamos C, Gust KR, Baboul AG, Heeg MJ, Schlegel HB, Winter CH. Inorg Chem. 2001;40:6451–62.
22. Fulias A, Vlase G, Grigorie C, Ledeţi I, Albu P, Bilanin M, Vlase T. Thermal behaviour studies of procaine and benzocaine. J Therm Anal Calorim. 2013;113(1):265–71.
23. Fuliaş A, Ledeţi I, Vlase G, Vlase T. Physico-chemical solid-state characterization of pharmaceutical pyrazolones: an unexpected thermal behaviour. J Pharm Biomed Anal. 2013;81–82:44–9.
24. Ledeţi I, Simu G, Vlase G, Săvoiu G, Vlase T, Şuta L-M, Popoiu C, Fuliaş A. Synthesis and solid-state characterization of Zn(II) metal complex with acetaminophen. Rev Chim-Bucharest. 2013;64(10):1127–30.
25. Fuliaş A, Vlase G, Vlase T, Soica C, Heghes A, Craina M, Ledeti I. Comparative kinetic analysis on thermal degradation of some cephalosporins using TG and DSC data. Chem Cent J. 2013;7:70.
26. Fuliaş A, Popoiu C, Vlase G, Vlase T, Onetiu D, Savoiu G, Simu G, Patrutescu C, Ilia G, Ledeti I. Thermoanalytical and spectroscopic study on methotrexate: active substance and tablet. Dig J Nanomater Bios. 2014;9:93–8.
27. Ledeti I, Fulias A, Vlase G, Vlase T, Doca N. Novel triazolic copper (II) complex: synthesis, thermal behaviour and kinetic study. Rev Roum Chim. 2013;58:441–50.
28. Ledeti I, Vlase T, Vlase G, Suta LM, Fulias A, Belu I. Synthesis and solid-state characterization of a cobalt(II) triazolic complex. Rev Chim-Bucharest. 2014;65:897–902.
29. Venter MM, Cîntă Pînzaru S, Haiduc I, Bercean V. FT-IR and FT-Raman studies on new 5-mercapto-1,3,4-thiadiazole-2yl carboxylic derivatives. Studia Univ Babes-Bol Physica. 2004;XLYX(3):285–8.
30. Venter MM, Bercean VN, Ilici M, Cîntă Pînzaru S, Chiş V, Haiduc I. Synthesis and vibrational studies on new complexes of monodeprotonated (5-mercapto-1,3,4-thiadiazole-2-yl)thioacetic acid. Studia Univ Babes-Bol Chem. 2006;LI:65–71.
31. Venter MM, Bercean VN, Ilici M, Cîntă Pînzaru S. New metal complexes of monoanionic (3*H*-2-tioxo-1,3,4-thiadiazol-5-il)-thioacetic acid. X-ray structure of $[Na(C_2N_2HS_3CH_2COO)(H_2O)_4]_2 \times 2H_2O$. Rev Roum Chim. 2007;52:75–9.
32. Venter MM, Bercean VN, Varga R, Sasca V, Petrişor T, Ciontea L. Solid state structure of a new nickel(ii)(3*H*-2-thioxo-1,3,4-thiadiazol-2-yl)thioacetato complex. Studia Univ Babes-Bolyai Chem. 2010;XLV:217–26.
33. Friedman HL. Kinetics of thermal degradation of char-foaming plastics from thermogravimetry: application to a phenolic resin. J Polym Sci. 1965;6C:183–95.
34. Flynn JH, Wall LA. A quick, direct method for the determination of activation energy from thermogravimetric data. Polym Lett. 1966;4:323–8.
35. Ozawa T. A new method of analyzing thermogravimetric data. Bull Chem Soc Jpn. 1965;38:1881–6.
36. Murray P, White J. Kinetics of thermal dehydration of clays: IV. Interpretation of differential thermal analysis of the clay mineral. Trans Brit Ceram Soc. 1955;54:204–38.
37. Kissinger HE. Reaction kinetics in differential thermal analysis. Anal Chem. 1957;29(11):1702–6.
38. Akahira T, Sunose T (1971) Trans. Joint convention of four electrical institutes, paper no. 246 (1969) research report, chiba institute of technology. Sci Technol 16: 22–31
39. Doyle CD. Estimating isothermal life from thermogravimetric data. J Appl Sci. 1962;6:639–46.
40. Serra R, Nomen R, Sempere J. The non-parametric kinetics. A new method for the kinetic study of thermoanalytical data. J Therm Anal Calorim. 1998;52:933–43.
41. Serra R, Sempere J, Nomen R. A new method for the kinetic study of thermoanalytical data: the non-parametric kinetics method. Thermochim Acta. 1998;316:37–45.
42. Vlase T, Vlase G, Doca N, Ilia G, Fuliaş A. Coupled thermogravimetric-IR techniques and kinetic analysis by non-isothermal decomposition of Cd^{2+} and Co^{2+} vinyl-phosphonates. J Therm Anal Calorim. 2009;97:467–72.
43. Vlase T, Vlase G, Birta N, Doca N. Comparative results of kinetic data obtained with different methods for complex decomposition steps. J Therm Anal Calorim. 2007;88:631–5.
44. Wall ME. Singular value decomposition and principal component analysis. In: Berrar DP, Dubitzky W, Granzow M, editors. A practical approach to microarray data analysis. Boston: Kluwer-Norwel; 2003. p. 91–109.
45. Šesták J, Berggren G. Study of the kinetics of the mechanism of solid-state reactions at increasing temperatures. Thermochim Acta. 1971;3:1–12.